

# Monopole effects, core excitations, and $\beta$ decay in the $A = 130$ hole nuclei near $^{132}\text{Sn}^*$

Han-Kui Wang(王韩奎)<sup>1,1)</sup> Zhi-Hong Li(李志宏)<sup>2</sup> Cen-Xi Yuan(袁岑溪)<sup>3</sup> Zhi-Qiang Chen(陈志强)<sup>4</sup>  
Ning Wang(王宁)<sup>1</sup> Wei Qin(秦伟)<sup>1</sup> Yi-Qi He(何翊绮)<sup>5</sup>

<sup>1</sup>College of Physics and Telecommunication Engineering, Zhoukou Normal University, Henan 466000, China

<sup>2</sup>China Institute of Atomic Energy, P.O. Box 275(10), Beijing 102413, China

<sup>3</sup>Sino-French Institute of Nuclear Engineering and Technology Sun Yat-Sen University, Zhuhai 519082, China

<sup>4</sup>School of Physics and State Key Laboratory of Nuclear Physics and Technology, Peking University, Beijing 100871, China

<sup>5</sup>College of mathematics and statistics, Zhoukou Normal University, Henan 466000, China

**Abstract:** The proton and neutron cross-shell excitations across the  $Z = 50$  shell are investigated in the southwest quadrant of  $^{132}\text{Sn}$  by large-scale shell-model calculations with extended pairing and multipole-multipole force. The model space allows proton (neutron) core excitations, and both the low- and high-energy states for  $^{130}\text{In}$  are well described, as found by comparison with the experimental data. The monopole effects between the proton orbit  $g_{9/2}$  and neutron orbit  $g_{7/2}$  are studied as the new monopole correction that perfectly reproduces the first  $1^+$  level in  $^{130}\text{In}$ . The energy interval of proton (neutron) core excitations in  $^{130}\text{In}$  lies in the range of 4.5–6.5 (2.0–4.1) MeV, and the high energy yrast states are predicted as neutron core excitations. The  $\beta$  decays are calculated among the  $A=130$  nuclei of  $^{130}\text{In}$ ,  $^{130}\text{Sn}$  and  $^{130}\text{Cd}$ .

**Keywords:** monopole effects, core-excitations,  $\beta$  decay, hole nuclei

**PACS:** 21.10.-k, 21.60.Cs, 21.30.Fe     **DOI:** 10.1088/1674-1137/43/5/054101

## 1 Introduction

The study of nuclear structure of neutron rich nuclei near the  $A = 130$  mass region is fundamentally important for both nuclear physics and astrophysics. The classical  $N = 82$   $r$ -process waiting-point nuclide  $^{130}\text{Cd}$  was first identified by Kratz et al. in 1986 at CERN/ISOLDE [1]. The  $\beta$  decay of the semi-magic nucleus  $^{130}\text{Cd}$  has been studied at the RIBF facility at the RIKEN Nishina Center, and the energy of the first excited  $1^+$  state of  $^{130}\text{In}$  at 2120 keV was confirmed in Ref. [2]. The shell-model calculations produce the  $1^+$  level by undervaluation of 550–750 keV [3, 4]. The obvious difference between shell model theory and experiment was improved by introducing monopole corrections to the employed Hamiltonian [5].

The monopole interaction plays not only a significant role in the shell evolution owing to the monopole shift when valence nucleons occupy certain orbits [6], but also modifies the high core excitations in hole nuclei close to doubly magic  $^{132}\text{Sn}$  [7]. The core excitation is crucial for studying high energy levels in nuclei close to doubly magic  $^{132}\text{Sn}$ . For example, the  $17/2^+$  level is well described as a core-

excited isomer with  $T_{1/2} = 630(60)\text{ns}$  in  $^{131}\text{In}$  [8]. Besides the core excitations, the  $\beta$  decay also plays an important role in nuclear physics, astrophysics and particle physics, and provides crucial information about the shell-model interaction and nuclear properties. The shell model calculations were performed to determine the half-lives and neutron-branching probabilities of the  $r$ -process waiting-point nuclei at the magic neutron number  $N = 82$ , and a good account of all experimentally known half-lives and  $Q$ -values is given for these  $N = 82$   $r$ -process waiting-point nuclei [5]. Recently, some frameworks found that the tensor force and particle-vibration coupling play important roles in the beta-decay calculations [9–11], which provide valuable improvements for further shell-model research.

The doubly magic nuclei are very important for the study of nuclear structure. The prompt and delayed  $\gamma$ -cascades in doubly magic  $^{132}\text{Sn}$  and its neighboring  $^{131}\text{Sn}$  have been studied at GAMMASPHERE using the  $^{248}\text{Cm}$  fission source [12]. By direct observation of single-particle states in odd-mass isotopes close to  $^{132}\text{Sn}$ , the doubly magic nature of  $^{132}\text{Sn}$  has been reconfirmed [13, 14]. As a strong signal of shell closure, the validity of the seniority has

Received 24 December 2018, Revised 18 February 2019, Published online 2 April 2019

\* Research at Zhoukou Normal University is supported by the National Natural Science Foundation of China (11505302). Research at China Institute of Atomic Energy is supported by the National Natural Science Foundation of China (11490563) and by the National Key Research and Development Program of China (2016YFA0400502). Research at Sun Yat-Sen University is supported by the National Natural Science Foundation of China (11775316)

1) E-mail: whk2007@163.com

©2019 Chinese Physical Society and the Institute of High Energy Physics of the Chinese Academy of Sciences and the Institute of Modern Physics of the Chinese Academy of Sciences and IOP Publishing Ltd

been predicted in earlier theoretical calculations and confirmed through experimental observation of  $8^+$  seniority isomeric states in  $^{126}\text{Pd}$ ,  $^{128}\text{Pd}$  and  $^{130}\text{Cd}$  [2, 15]. Further shell-model calculations are performed on these, and it was concluded that the shell closure persists at the neutron number  $N = 82$  in the neutron-rich region [16]. For the neutron-rich nuclei close to  $^{132}\text{Sn}$ , the extended pairing-plus-quadrupole model with monopole corrections (EPQQM) [17-20] provides a method to accurately describe both low-lying states and core excitations in a consistent manner [7, 16, 21].

In the present work, the EPQQM are applied to the hole nuclei at the southwestern quadrant of  $^{132}\text{Sn}$  to study the monopole effects and core excited states by large-scale shell-model calculations. The model space consists of five neutron orbits ( $0g_{7/2}, 1d_{5/2}, 2s_{1/2}, 0h_{11/2}, 1d_{3/2}$ ) and four proton orbits ( $0f_{5/2}, 1p_{3/2}, 1p_{1/2}, 0g_{9/2}$ ) with  $^{78}\text{Ni}$  as the closed core. In addition, two neutron orbits ( $1f_{7/2}, 2p_{3/2}$ ) above the  $N = 82$  shell gap and two proton orbits ( $0g_{7/2}, 1d_{5/2}$ ) above the  $Z = 50$  shell gap are included for allowing both proton and neutron core excitations. The proton (neutron) core excitations were restricted, such that only one proton (neutron) was allowed to excite across the  $Z = 50$  ( $N = 82$ ) shell gap. The single-particle energies and the two-body force strengths employed in the present work are consistent with our previous paper [21, 22]. The proton core excitations (PCE) are firstly discussed in the hole nuclei close to  $^{132}\text{Sn}$ . The monopole effects and neutron core excitations (NCE) will also be discussed in the present work. The  $\beta$  decays among  $^{130}\text{Cd}$ ,  $^{130}\text{In}$  and  $^{130}\text{Sn}$  are studied with the quenching factor 0.7. The experimental data are obtained partly from the ENSDF database of NNDC On-line Data Service with cut-off dates of May 11, 2001, May 31, 2008, and May 31, 2008 for  $^{130}\text{Sn}$ ,  $^{130}\text{Cd}$ , and  $^{130}\text{In}$  respectively. The shell-model code NUSHELLX@MSU is used for calculations [23].

## 2 The Hamiltonian and modifications

With the proton-neutron ( $pn$ ) representation, the EPQQM Hamiltonian [17-20] is given as follows:

$$\begin{aligned}
 H &= H_{\text{sp}} + H_{P_0} + H_{P_2} + H_{Q_0} + H_{O_0} + H_{HH} + H_{\text{mc}} \\
 &= \sum_{\alpha,i} \varepsilon_{\alpha}^i c_{\alpha,i}^{\dagger} c_{\alpha,i} - \frac{1}{2} \sum_{J=0,2} \sum_{i\bar{i}} g_{J,i\bar{i}} \sum_M P_{JM,i\bar{i}}^{\dagger} P_{JM,i\bar{i}} \\
 &\quad - \frac{1}{2} \sum_{i\bar{i}} \frac{\chi_{2,i\bar{i}}}{b^4} \sum_M : Q_{2M,i\bar{i}}^{\dagger} Q_{2M,i\bar{i}} : \\
 &\quad - \frac{1}{2} \sum_{i\bar{i}} \frac{\chi_{3,i\bar{i}}}{b^6} \sum_M : O_{3M,i\bar{i}}^{\dagger} O_{3M,i\bar{i}} : \\
 &\quad - \frac{1}{2} \sum_{i\bar{i}} \frac{\chi_{4,i\bar{i}}}{b^8} \sum_M : H_{4M,i\bar{i}}^{\dagger} H_{4M,i\bar{i}} : \\
 &\quad + \sum_{a \leq c, i\bar{i}'} k_{\text{mc}}(ia, i'c) \sum_{JM} A_{JM}^{\dagger}(ia, i'c) A_{JM}(ia, i'c). \quad (1)
 \end{aligned}$$

Equation (1) includes the single-particle Hamiltonian ( $H_{\text{sp}}$ ), the  $J = 0$  and  $J = 2$  pairing ( $P_0^{\dagger}P_0$  and  $P_2^{\dagger}P_2$ ), the quadrupole-quadrupole ( $Q^{\dagger}Q$ ), the octupole-octupole ( $O^{\dagger}O$ ), the hexadecapole-hexadecapole ( $H^{\dagger}H$ ) terms, and the monopole corrections ( $H_{\text{mc}}$ ). In the  $pn$ -representation,  $P_{JM,i\bar{i}}^{\dagger}$  and  $A_{JM}^{\dagger}(ia, i'c)$  are the pair operators, while  $Q_{2M,i\bar{i}}^{\dagger}$ ,  $O_{3M,i\bar{i}}^{\dagger}$  and  $H_{4M,i\bar{i}}^{\dagger}$  are the quadrupole, octupole, and hexadecapole operators, respectively, where  $i$  ( $i'$ ) depict the indices for protons (neutrons). The parameters  $g_{J,i\bar{i}}$ ,  $\chi_{2,i\bar{i}}$ ,  $\chi_{3,i\bar{i}}$ ,  $\chi_{4,i\bar{i}}$ , and  $k_{\text{mc}}(ia, i'c)$  are the corresponding force strengths, and  $b$  is the harmonic-oscillator range parameter. The two-body force strengths that suit the present particle-hole model space are listed in Table 1.

Table 1. Two-body force strengths (in MeV) used in the present calculation.

$i\bar{i}'$	$g_{0,i\bar{i}'}$	$g_{2,i\bar{i}'}$	$\chi_{2,i\bar{i}'}$	$\chi_{3,i\bar{i}'}$	$\chi_{4,i\bar{i}'}$
$pp$	0.136	0.038	0.102	0.032	0.0015
$nn$	0.117	0.035	0.140	0.004	0.0008
$pn$	0	0	0.082	0	0.0009

In our previous papers, the monopole corrections of  $M_{c1} \equiv k_{\text{mc}}(\nu h_{11/2}, \nu f_{7/2}) = 0.52$  MeV and  $M_{c2} \equiv k_{\text{mc}}(\pi g_{9/2}, \nu h_{11/2}) = -0.4$  MeV are employed to modify the  $N = 82$  shell gap. The  $M_{c2}$  is also necessary for obtaining the right ground state of  $^{129}\text{Cd}$  [22]. The  $M_{c3} \equiv k_{\text{mc}}(\pi g_{9/2}, \nu g_{7/2}) = -1.0$  MeV is the new monopole correction introduced in the present work. As shown in Fig. 1, adding the monopole corrections of  $M_{c1}$  and  $M_{c2}$  has no influence on low-lying levels of  $^{130}\text{Sn}$  and  $^{130}\text{Cd}$ , while the  $M_{c2}$  shifts up the  $3^+$ ,  $5^+$  and  $1^+$  levels in  $^{130}\text{In}$ . The fact that the datum  $1^+$  level at 2.120 MeV is much lower than the theoretical value in the present work is the experimental base for adding  $M_{c3}$ . The orbit  $\pi g_{9/2}$  ( $\nu g_{7/2}$ ) is full of particles in the configuration of low-lying levels at  $^{130}\text{Sn}$  ( $^{130}\text{Cd}$ ), however the  $M_{c3} \equiv k_{\text{mc}}(\pi g_{9/2}, \nu g_{7/2})$  has effects only when the orbits  $\pi g_{9/2}$  and  $\nu g_{7/2}$  are both lacking particles, as in the  $1^+$  level with a configuration of  $\pi g_{9/2}^{-1} \nu g_{7/2}^{-1}$  in  $^{130}\text{In}$ . Hence, the Hamiltonian including  $M_{c3}$  has no effects on low-lying levels of  $^{130}\text{Sn}$  and  $^{130}\text{Cd}$ , however it significantly shifts down the  $1^+$  level in  $^{130}\text{In}$ . This represents a neat reduction of the theoretical value and the corresponding datum. Unlike the addition of  $M_{c1}$  and  $M_{c2}$  to modify high core-excitations [7], the purpose of adding  $M_{c3}$  is not for core excitation, as no effect was found on core excitations mentioned in the present work by adding  $M_{c3}$ .

The matrix element of  $J = 4$  in the proton orbit  $g_{9/2}$  is increased by  $-0.18$  MeV to obtain the right order of  $6^+$  and  $8^+$  levels in  $^{128}\text{Pd}$  [16]. For simplified notation, this modification is marked as  $M_{e1}$ . As shown in Fig. 1(a), although the  $M_{e1}$  has no effects on the low-lying levels of

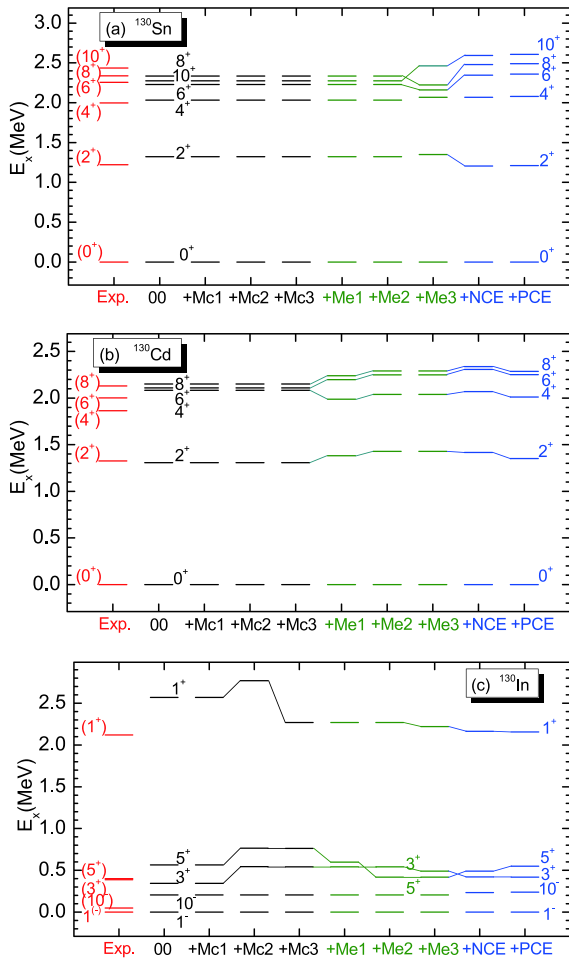


Fig. 1. (color online) Effects of monopole corrections ( $M_c$ ), matrix element ( $M_e$ ) modifications and allowing the neutron (proton) core excitations (NCE & PCE) in the low-lying levels of hole nuclei  $^{130}\text{Sn}$ ,  $^{130}\text{Cd}$  and  $^{130}\text{In}$  in comparison with corresponding data. The  $M_c$  and  $M_e$  are added to the initial Hamiltonian (00) one by one, and their definition and value of the  $M_c$  and  $M_e$  are given in the text.

$^{130}\text{Sn}$ , it breaks the degeneracy in  $4^+$ ,  $6^+$ , and  $8^+$  levels of  $^{130}\text{Cd}$ , and also shifts down the  $5^+$  level in  $^{130}\text{In}$  to close to the corresponding datum in the experiment. In the research of the  $A = 129$  hole nuclei near  $^{132}\text{Sn}$ , two zero-value matrix elements were given new values in the Hamiltonian (marked as  $M_e2$ ),  $\langle p_{1/2}, g_{9/2}, |V|p_{1/2}, g_{9/2}, \rangle_{J=4}^\pi = 0.32$  and  $\langle p_{1/2}, g_{9/2}, |V|p_{1/2}, g_{9/2}, \rangle_{J=5}^\pi = -0.22$ . The  $M_e2$  has no effects on the low-lying levels of  $^{130}\text{Sn}$ , and little effect on  $^{130}\text{Cd}$ . It has obvious effects on shifting down the  $5^+$  level in  $^{130}\text{In}$ . During the study of Sb isotopes in the particle-hole nuclei near  $^{132}\text{Sn}$ , the new modification is needed in the three interaction matrix elements (marked as  $M_e3$ ) by the amount of  $\Delta\langle h_{11/2}, h_{11/2} | V | h_{11/2}, h_{11/2} \rangle^v = -0.15, -0.15, +0.2$  (MeV) for  $J = 6, 8, 10$ , respectively. Although the  $M_e3$  is used in the northeastern quadrant of  $^{132}\text{Sn}$  [24], it also works well in the present hole-nuclei region. As shown in Fig. 1(a), the  $M_e3$  not only breaks the

degeneracy in  $6^+$ ,  $8^+$  and  $10^+$  levels in  $^{130}\text{Sn}$ , but also gives the consistent order with experimental data.

### 3 The proton (neutron) core excitations and the $\beta$ decay

The core excitations depict one of most important physics effects in the hole-nuclei region near  $^{132}\text{Sn}$ . In low-lying levels of  $^{130}\text{Sn}$  (Fig. 1(a)), including neutron core-excitations, the  $2^+$  level is shifted down, and the  $6^+$ ,  $8^+$ , and  $10^+$  levels are lifted up. The model space allowing neutron core excitations keeps the level order consistent with the experimental ( $3^+$ ) and ( $5^+$ ) states in  $^{130}\text{In}$ . After adding these modifications to the Hamiltonian, we study the data in  $^{130}\text{In}$  [2] by the model space allowing both proton and neutron core excitations. As shown in Fig. 2(a), the low-lying states are accurately described by the new Hamiltonian with  $M_c3$  and  $M_e3$  modifications. The  $1^+$  level with 2.120 MeV is the main final state for the  $\beta$  decay of  $^{130}\text{Cd}$  that occurs in about 70% of all decays [2], and the theoretical one at 2.155 MeV is a perfect reproduction with the main configuration of  $\pi g_{9/2}^{-1} \nu g_{7/2}^{-1}$ .

The  $1^+$  levels exhibited in Fig. 2(b) are the core excitations. With the exception of the highest one near 6 MeV, which is the proton core excited state across the  $Z = 50$  shell gap with configuration of  $\pi g_{9/2}^{-2} g_{7/2} \nu d_{3/2}^{-1}$ , the others are the neutron core excitations across the  $N = 82$  shell gap. Their main configurations are  $\pi g_{9/2}^{-1} \nu h_{11/2}^{-1} d_{3/2}^{-1} f_{7/2}$ ,  $\pi p_{1/2}^{-1} \nu h_{11/2}^{-2} f_{7/2}$ ,  $\pi p_{3/2}^{-1} \nu h_{11/2}^{-2} f_{7/2}$ , and  $\pi f_{5/2}^{-1} \nu h_{11/2}^{-2} f_{7/2}$ . Their proton configurations are marked in Fig. 2(b) for the purposes of differentiating between them. Fig. 3 shows the lowest core-excitations in  $^{130}\text{In}$ . The NCE states lie lower with the energy interval 2.0–4.1 MeV. The latest observed decays with the energy interval 3.5–4.3 MeV have a large overlap. The PCE states have the energy interval of 4.5–6.5 MeV, which spans the energy interval 5.2–5.6 MeV of the newly observed decays in  $^{130}\text{In}$ .

For the positive parity states of  $^{130}\text{In}$  in Fig. 3(a), the ones of NCE from  $0^+$  to  $7^+$  have the main configuration of  $\pi p_{1/2}^{-1} \nu h_{11/2}^{-2} f_{7/2}$ , and the last three levels of  $8^+$ ,  $9^+$ , and  $10^+$  have the main configuration of  $\pi g_{9/2}^{-1} \nu h_{11/2}^{-1} d_{3/2}^{-1} f_{7/2}$ , while the  $9^+$  and  $10^+$  levels at 3.883 and 3.804 MeV, respectively, depict the yrast state in theory. The higher positive parity states of PCE also have two main configurations, the  $\pi p_{1/2}^{-1} g_{9/2}^{-1} g_{7/2} \nu h_{11/2}^{-1}$  is for the levels of  $0^+$ ,  $5^+$ ,  $8^+$ ,  $9^+$ , and  $10^+$ , and the  $\pi g_{9/2}^{-2} g_{7/2} \nu d_{3/2}^{-1}$  is for the last six levels. The negative parity states of NCE only have a single configuration  $\pi g_{9/2}^{-1} \nu h_{11/2}^{-2} f_{7/2}$ , and the PCE with negative parity have the main configuration of  $\pi g_{9/2}^{-2} g_{7/2} \nu h_{11/2}^{-1}$ , except for the  $1^-$  level with configuration of  $\pi p_{1/2}^{-1} g_{9/2}^{-1} g_{7/2} \nu d_{3/2}^{-1}$ .

As shown in Fig. 4, the energy interval in  $^{130}\text{Sn}$  is 3.8–5.4 MeV (5.7–7.7 MeV) for neutron (proton) core

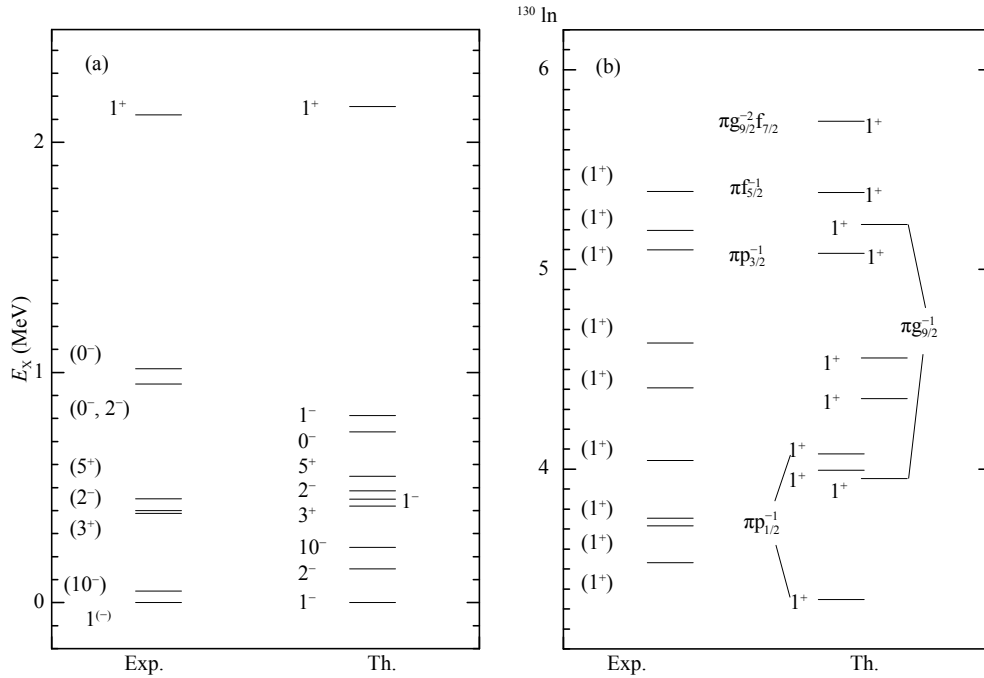


Fig. 2. Level scheme of  $^{130}\text{In}$  under the Hamiltonian including  $M_{c3}$  and  $M_e3$  in comparison with corresponding data. The proton configurations of  $1^+$  levels in part (b) are provided. The experimental data are obtained from the ENSDF database of NNDC On-line Data Service with cut-off dates of May 11, 2001, May 31, 2008, and May 31, 2008 for  $^{130}\text{Sn}$ ,  $^{130}\text{Cd}$ , and  $^{130}\text{In}$  respectively, with the exception of  $(2^-)$ ,  $(1^-, 2^-)$ ,  $(0^-)$  and  $(1^+)$  levels in the energy interval 3.5–4.1 MeV [2].

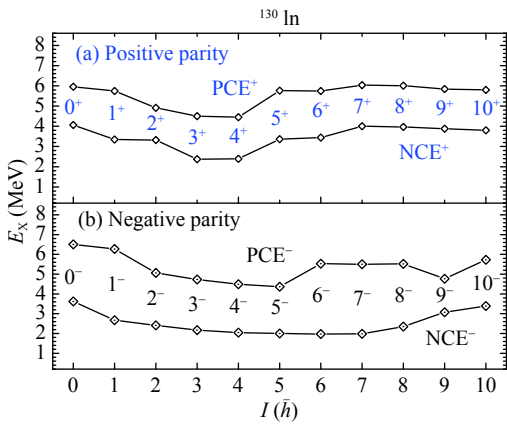


Fig. 3. (color online) Neutron (proton) core-excited states in  $^{130}\text{In}$ . "I" is used to mark the level spin.

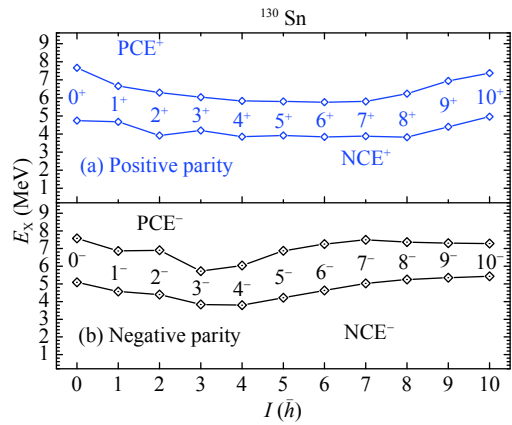


Fig. 4. (color online) Neutron (proton) core-excited states in  $^{130}\text{Sn}$ . "I" is used to mark the level spin.

excitations, which is obviously higher than the one in  $^{130}\text{In}$ . For the neutron core excitations, the positive parity states have the main configuration of  $\nu h_{11/2}^{-3} f_{7/2}$ , while the  $8^+$  level is the lowest one with 3.824 MeV and the  $10^+$  state is the highest one with 4.966 MeV. The negative parity levels have the main configuration of  $\nu h_{11/2}^{-2} d_{3/2}^{-1} f_{7/2}$ , while the lowest one is the  $4^-$  level at 3.793 MeV and the highest one is the  $8^-$  level at 5.253 MeV. The  $5^+$ ,  $7^+$ ,  $9^+$ ,  $0^-$ ,  $1^-$ , and  $10^-$  levels are the yrast states in theory. For the proton core excitations, the positive parity ones have the main configuration of  $\pi g_{9/2}^{-1} g_{7/2} \nu h_{11/2}^{-2}$ , while the  $0^+$  ( $6^+$ ) level is the highest (lowest) one with 7.668 (5.765) MeV.

The negative parity states of proton core excitations have two main configurations, which are  $\pi g_{9/2}^{-1} g_{7/2} \nu h_{11/2}^{-2}$  is for the levels of  $0^-$ ,  $7^-$ ,  $8^-$ ,  $9^-$  and  $10^-$  and  $\pi p_{1/2}^{-1} g_{7/2} \nu h_{11/2}^{-1} d_{3/2}^{-1}$  for the levels from  $1^-$  to  $6^-$ .

The proton core excitations in  $^{130}\text{Cd}$  (Fig. 5) have a much higher energy interval (6.2–9.5 MeV), where the main configuration is  $\pi g_{9/2}^{-3} g_{7/2}$  for the positive parity and  $\pi p_{1/2}^{-1} g_{9/2}^{-2} g_{7/2}$  for the negative. The energy interval of neutron excitations is 3.7–5.7 MeV, while their main configuration is  $\pi g_{9/2}^{-2} \nu h_{11/2}^{-1} f_{7/2}$  for the positive parity levels. The negative parity of neutron core excitations have two

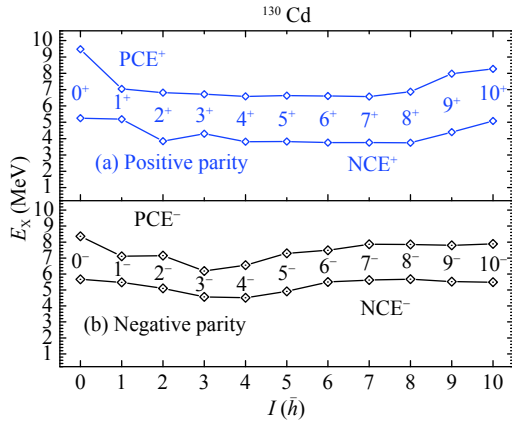


Fig. 5. (color online) Neutron (proton) core-excited states in  $^{130}\text{Cd}$ . "I" is used to mark the level spin.

main configurations,  $\pi g_{9/2}^{-2} \nu d_{3/2}^{-1} f_{7/2}$  for the levels from  $2^-$  to  $5^-$  and  $\pi p_{1/2}^{-1} g_{9/2}^{-1} \nu h_{11/2}^{-1} f_{7/2}$  for the others. The ten neutron core excitations of  $3^+$ ,  $5^+$ ,  $7^+$ ,  $9^+$ ,  $10^+$ ,  $0^-$ ,  $1^-$ ,  $8^-$ ,  $9^-$ , and  $10^-$  are the yrast states in theory.

In contrast to electromagnetic transitions,  $\beta$  decay accompanies charge-changing from one nucleus to another. The study of  $\beta$  decay shows the nature of both the weak interaction and the structure of nuclear wave functions. The  $\beta$  decays among the  $A = 130$  nuclei of  $^{130}\text{Cd}$ ,  $^{130}\text{In}$  and  $^{130}\text{Sn}$  are studied in the present work (Fig. 6). The quenching factor is selected as 0.7, and the theoretical results provide a good performance. The properties of the  $\beta$  decay in the classical  $N = 82$  waiting point nucleus  $^{130}\text{Cd}$  play an important role in the calculations of the astrophysical  $r$ -process.

The Gamow-Teller transition from the  $(0^+)$  ground state of  $^{130}\text{Cd}$  to the  $1^+$  level with 2.120 MeV in  $^{130}\text{In}$  dominates about 70% of the  $\beta$  decays in  $^{130}\text{Cd}$ . If only GT transitions are considered, this branching ratio is larger than 99% in the present work. The half-life of  $^{130}\text{Cd}$  is 36 ms, also dominated by this GT transition. The  $jj45\text{pna}$  interaction is used for comparison, and is in approximate accordance with our results. The contribution of the first forbidden transition is small, about 13% [25]. As shown in Fig. 6(a), by comparing with corresponded datum from ground state of  $^{130}\text{Cd}$  to the  $1^+$  level with 2.120 MeV in  $^{130}\text{In}$ , the theoretical  $\log ft$  value of the GT transition is smaller with the normal quenching factor (0.7). When 0.4 is used as quenching factor, the half-life of  $^{130}\text{Cd}$  will be efficiently reproduced. By Using the newly developed fully self-consistent proton-neutron quasiparticle random phase approximation (RQRPA), the half-life of  $^{130}\text{Cd}$  was well reproduced in comparison with experimental datum [26, 27].

Note that the ground state of  $^{130}\text{Cd}$  is dominated by  $\pi g_{9/2}^{-2}$  (about 80%), while the  $1^+$  level with 2.120 MeV in  $^{130}\text{In}$  is dominated by  $\pi g_{9/2}^{-1} \nu g_{7/2}^{-1}$ . The GT transition is

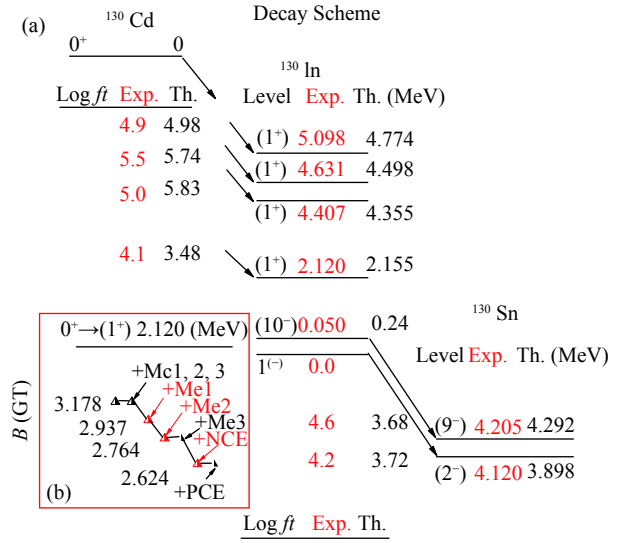


Fig. 6. (color online)  $\beta$  decay among the  $A = 130$  nuclei of  $^{130}\text{Cd}$ ,  $^{130}\text{In}$  and  $^{130}\text{Sn}$ . The effects of modifications  $M_c$  and  $M_e$  (added to the Hamiltonian one by one) on the value of the reduced Gamow-Teller transition probability (B(GT)) to  $(1^+)$  with 2.120 MeV. Experimental data are obtained from the ENSDF database of NNDC On-line Data Service with cut-off dates of May 11, 2001, May 31, 2008, and May 31, 2008 for  $^{130}\text{Sn}$ ,  $^{130}\text{Cd}$ , and  $^{130}\text{In}$  respectively.

rather strong between these two configurations, so the  $\log ft$  value becomes rather small, and is very close to the super-allowed transition. Apart from this exception, the decay to the other  $1^+$  states in  $^{130}\text{In}$  becomes more difficult with larger  $\log ft$  in both experiment and theory.

By adding the above modifications to the Hamiltonian one by one, the effects of them on B(GT) to  $(1^+)$  at 2.120 MeV are exhibited in Fig. 6(b). The three monopole corrections of  $M_c1$ ,  $M_c2$ , and  $M_c3$  have no effects on this B(GT), while the matrix modifications of  $M_e1$  and  $M_e2$  obviously exert an influence on it. The model space allowing neutron core excitations also decreases the value of B(GT) in Fig. 6. As a mother nucleus, the  $\beta$  decay from  $^{130}\text{In}$  forms the semi-magic nucleus  $^{130}\text{Sn}$ . Although the  $9^-$  and  $2^-$  states in  $^{130}\text{Sn}$  are located relatively high, there is less possibility for them to be core excitation states by comparing with the present calculations. More studies are expected to clarify the contribution of core excitation on the  $\beta$  decay in the southwestern quadrant of  $^{132}\text{Sn}$ .

## 4 Summary

In summary, the core excitations and the monopole effects are discussed in the neutron-rich hole nuclei close to  $^{132}\text{Sn}$  by large-scale shell-model calculations. The model space includes five neutron orbits ( $0g_{7/2}, 1d_{5/2}, 2s_{1/2}, 0h_{11/2}, 1d_{3/2}$ ) and four proton orbits ( $0f_{5/2}, 1p_{3/2},$

$1p_{1/2}, 0g_{9/2}$ ), while two neutron orbits ( $1f_{7/2}, 2p_{3/2}$ ) above the  $N = 82$  shell gap and two proton orbits ( $0g_{7/2}, 1d_{5/2}$ ) above the  $Z = 50$  shell gap are considered for allowing both proton and neutron core excitations. The main conclusions in the present work are the following.

The monopole corrections and matrix element modifications employed in our previous papers are checked carefully by the odd-odd nucleus  $^{130}\text{In}$  and even-even nuclei of  $^{130}\text{Sn}$  and  $^{130}\text{Cd}$ . The new monopole effect of  $M_{c3}$  is found between the proton orbit  $g_{9/2}$  and neutron

orbit  $g_{7/2}$  in hole-nuclei close to doubly magic  $^{132}\text{Sn}$ . The energy intervals of proton and neutron core excitations in  $^{130}\text{In}$  lie in the energy range of 4.5–6.5 MeV and 2.0–4.1 MeV, respectively. Neutron core excitations the high energy yrast states are found theoretically in the  $A = 130$  nuclei of  $^{130}\text{In}$ ,  $^{130}\text{Sn}$  and  $^{130}\text{Cd}$ . The  $\beta$  decay among these  $A = 130$  nuclei are calculated in the present work. The dominant  $\beta$  decays in  $^{130}\text{Cd}$ , the Gamow-Teller transition to the  $1^+$  level with 2.120 MeV in  $^{130}\text{In}$  is discussed in detail.

## References

- 1 K. L. Kratz, H. Gabelmann, W. Hillebrandt et al, *Z. Phys. A*, **325**: 489 (1986)
- 2 A. Jungclaus, H. Grawe, S. Nishimura et al, *Phys. Rev. C*, **94**: 024303 (2016)
- 3 I. Dillmann, K. L. Kratz, A. Wöhr et al, *Phys. Rev. Lett.*, **91**: 162503 (2003)
- 4 G. Martínez-Pinedo and K. Langanke, *Phys. Rev. Lett.*, **83**: 4502 (1999)
- 5 J. J. Cuenca-García, G. Martínez-Pinedo, K. Langanke et al, *Eur. Phys. J. A*, **34**: 99 (2007)
- 6 T. Otsuka, T. Suzuki, R. Fujimoto et al, *Phys. Rev. Lett.*, **95**: 232502 (2005)
- 7 H. K. Wang, Y. Sun, Hua Jin et al, *Phys. Rev. C*, **88**: 054310 (2013)
- 8 M. Górska, L. Cáceres, H. Grawe et al, *Phys. Lett. B*, **672**: 313 (2009)
- 9 F. Minato and C. L. Bai, *Phys. Rev. Lett.*, **110**: 122501 (2013)
- 10 Y. F. Niu, Z. M. Niu, G. Colò et al, *Phys. Rev. Lett.*, **114**: 142501 (2015)
- 11 Y. F. Niu, Z. M. Niu, G. Colò et al, *Phys. Lett. B*, **780**: 325 (2018)
- 12 P. Bhattacharyya, P. J. Daly, C. T. Zhang et al, *Phys. Rev. Lett.*, **87**: 062502 (2001)
- 13 K. L. Jones, A. S. Adekola, D. W. Bardayan et al, *Nature (London)*, **465**: 454 (2010)
- 14 K. L. Jones, F. M. Nunes, A. S. Adekola et al, *Phys. Rev. C*, **84**: 034601 (2011)
- 15 H. Watanabe, G. Lorusso, S. Nishimura et al, *Phys. Rev. Lett.*, **111**: 152501 (2013)
- 16 H. K. Wang, K. Kaneko, and Y. Sun, *Phys. Rev. C*, **89**: 064311 (2014)
- 17 M. Hasegawa, K. Kaneko, and S. Tazaki, *Nucl. Phys. A*, **688**: 765 (2001)
- 18 K. Kaneko, M. Hasegawa, and T. Mizusaki, *Phys. Rev. C*, **66**: 051306(R) (2002)
- 19 K. Kaneko, Y. Sun, M. Hasegawa et al, *Phys. Rev. C*, **78**: 064312 (2008)
- 20 K. Kaneko, Y. Sun, T. Mizusaki et al, *Phys. Rev. C*, **83**: 014320 (2011)
- 21 Han-Kui Wang, Kazunari Kaneko, Yang Sun et al, *Phys. Rev. C*, **91**: 021303(R) (2015)
- 22 H. K. Wang, K. Kaneko, Y. Sun et al, *Phys. Rev. C*, **95**: 011304(R) (2017)
- 23 B. A. Brown and W. D. M. Rae, *Nucl. Data Sheets*, **120**: 115 (2014)
- 24 H. K. Wang, S. K. Ghorui, K. Kaneko et al, *Phys. Rev. C*, **96**: 054313 (2017)
- 25 Q. Zhi, E. Caurier, J. J. Cuenca-García et al, *Phys. Rev. C*, **87**: 025803 (2013)
- 26 Z. M. Niu, Y. F. Niu, H. Z. Liang et al, *Phys. Lett. B*, **723**: 172 (2013)
- 27 P. Möller, M. R. Mumpower, T. Kawano et al, *Atomic Data and Nuclear Data Tables* 125(2019)1-92